Journal of Civil Engineering and Materials Application
Journal home page: http://journals.lexispublisher.com/jcema

Received: 18 October 2017 • Accepted: 27 December 2017

Research

doi: 10.15412/J.JCEMA.12010304

Numerical Simulation of the Effect of Geometric Parameters of a Series of Attracting T-Shaped Spur Dikes on the Turbulent Flow Pattern

Iman Mirzaie[1]*, Amin Noori[2]

[1] Department of Civil Engineering, Graduate University of Advanced Technology, Kerman, Iran

[2] Department of Civil Engineering, Islamic Azad University of Rouzbahan, Sari, Iran

*Correspondence should be addressed to Iman Mirzaie, Department of Civil Engineering, Kerman Graduate University of Technology, Iran; Tell: +989131983062; Fax: +983432723320; Email: i.mirzaie@kgut.ac.ir.

ABSTRACT

Spur dike is a structure that extends transversely from the river bank toward its thalweg and deflects the flows away from the bank toward the center. One common type of this structure is the T-shaped spur dike, and the wings present in this dike can have major effects on the proximate flow pattern. In this study, the turbulent flow around three attracting T-shaped spur dikes placed in series was simulated using the FLUENT, the finite volume method and the k-ε turbulence model. The results of numerical modeling show that increasing the dike length and the spacing between dikes both alter the flow pattern around the structure, but flow pattern is more affected by the increase in the dike length than by the increase in the dike spacing.

Key words: T-shaped spur dike, Flow pattern, Finite volume, Fluent.

Journal of Civil Engineering and Materials Application is published by *Lexis Publisher*; Journal p-ISSN xxxx-xxxx; Journal e-ISSN 2588-2880.

1. INTRODUCTION

Assessment of riverbank erosion and its effects, such as the loss of riverside soil and damage to buildings constructed on the water's edge, are among the important applications of river engineering. Spur dike is a structure that extends transversely from the river bank toward its thalweg and deflects the flows away from the bank toward the center. Depending on its purpose, spur dike can be built as a single structure or as part of a series of consecutive structures placed on one side or both sides of the river. The result of flow deflection is the development of a flow separation zone with extreme turbulence around the dike and more extensively in its downstream. T-shaped spur dike is a common variant of the dike, whose unique shape can have major effects on the proximate flow pattern. Once reaching a spur dike, water develops eddy and turbulent currents, which need to be studied so as to predict the scour around the structure. Flow pattern around spur dikes has been the subject of many studies. The experiments of Fazli (2008) on straight spur dike placed on 90-degree bend showed that using two dikes instead on one is more effective in preventing the formation of secondary flow pattern and that this effect increases with the increase of the distance between them. They reported that in the presence of two spur dikes, the effect of the first dike on the flow pattern around the second one decreases with the increase of relative bend. They added that for three dikes placed in series with a spacing of 2.5 times the dike length, flow pattern between the first and second dikes is similar to the case when the third dike is not present, and the most important difference is in the near surface layer, where a strong reverse flow starts from the third dike and extends upstream-ward until reaching the zone between the first and second dikes (1). Elawady et al. (2001) studied the scour and flow pattern resulting from the blade spur dikes with different lengths (5, 10 and 15 cm), heights (2.5, 5 and 7.5 cm), degree of submergence (high and low submergence), and dike-bank angle (60, 90 and 120 degrees) placed in a straight channel with different discharge rates (73, 90, 104, 120, 145 and 180 liters per second) and two bed conditions (flatbed and equilibrium). According to their results, in the upstream side of the submerged dikes, near-bed flows exhibit upward vortices moving perpendicular to flow direction, which become downward at the downstream; while at the other layers, flow is mostly horizontal toward downstream.

But in the non-submerged dikes, near-bed flows rapidly pass beside the dike and there is no vortex in upstream (2). Vaghefi et al. (2009) performed an experimental study on T-shaped spur dikes placed individually and in series on a channel with a 90-degree bend. Variables of this study were the number of dikes, their position and spacing, dike length and length of its wing, and the curvature radius of the arch. According to study, a curvature radius of the arch decreases, scour hole extends toward downstream. At the upstream side of the dike, there are two separate groups of flow between its wing and the outer bank: upward flows starting from about mid-depth, which form a number of counterclockwise vortices with the axis perpendicular to the main flow direction, and their downward counterparts. The resultant of these two flows move out of the area between the dike wing and the outer bank toward the desired pressure. In the downstream side of the dike, reverse flows form counterclockwise vortices with an axis perpendicular to the main flow direction, which lead to reduced scouring in this area. When multiple dikes are placed in series, upstream and downstream flow patterns are the same as described above, and the presence of eddy currents and reverse flow between in the dikes can be generally expected. In the upstream side of an individual dike, there is a general increase in the size of vortices and separation zone from near-bed layer toward the surface (3). Vaghefi et al. (2015), numerically investigated the effect of submergence on the flow pattern around a T-shaped spur-dike located in the 90° bend. For this purpose, they used FLOW3D software and for verification used the experimental studies in the non-submerged state. The results showed that increase in the dimensions and number of vortices is associated with the submergence percentage. Also, the length and width of the separation zone in this case, were 1.6 times and 1.5 times the corresponding length and width of the separation zone in the case of non-submergence (4). Safarzadeh (2010) studied the flow pattern around the spur dikes of different shapes including the T-shaped dike. This study reported that adding fins to the straight spur dike can reduce or even eliminate the horseshoe vortex, protect the structure against high speed flows, and affect the shear stress distribution over the bed. It was also reported that in this type of spur dike, stress concentration decreases with the distance from the upstream nose, and stress distribution in the downstream side is far more uniform than the straight spur dike (5). Mehraein et al (2016) performed a laboratory study to examine the flow pattern and scour around T-shaped spur dike submerged in a 90-degree arc. These experiments investigated the effect of submergence (non-submerged, high and low submergence) and the radius of curvature (wide bend and sharp bend) on the flow lines in longitudinal and transverse sections, cross-sections at different heights, velocity profile, vortices, shear stress of the bed, turbulence intensity, and Reynolds stresses near the bed. In the scour pattern experiments, submergence percentage, Froude number, diameter of material, radius of curvature and location of the dike were analyzed. The results of this study showed that an increase in submergence percentage and decrease in the radius of curvature reduces the size of counterclockwise vortices, downward flow, and the length of reverse flow zone in the upstream side of the dike and increases the upward flow (6). Kuhnle et al. (2002, 2008), experimentally and numerically (using CCHE3D) investigated the flow pattern around a submerged trapezoidal shaped spur-dike with a straight alignment for two cases of the flatbed and scoured (balanced) bed. The results showed that the length of vortex zone from the flow separation point to the reattachment point is 1.6 L. The performed numerical simulation had acceptable results except for the recirculation zone downstream of the spur-dike and the maximum shear stress occurred downstream of the spur-dike and was 2.7 times the shear stress upstream of the spur-dike (7-9). Other research related to spur-dike include: Salamatian et al.(2016), Kumar and Malik (2016), Karami et al(2014), Yazdi et al. (2010), Duan et al.(2009), Tang et al.(2006), Ujitewaal (2005) Chen and Ikeda (1997) Osman et al. (1988) (10-18). Research show that flow pattern around a series of spur dikes depends on the spacing between them, flow rate, level of submergence, and geometry of placement. Although flow field around a single spur dike has been studied extensively, dikes are usually constructed in series so the flow pattern around multiple spur dikes placed in series needs further investigation. The present study employs FLUENT simulation based on finite volume method and the k-ε turbulence model to investigate the effect of geometric parameters of the T-shaped spur dike on the pattern of turbulent flow around three of these dikes.

2. THE GOVERNING EQUATIONS

The problem was modeled using finite volume method and the effect of turbulence was simulated with the k-ε model. The rules governing the incompressible viscous fluid flow are expressed by one continuity equation and three momentum equations (along with the three coordinate axes) known as Navier-Stokes equations. In fact, these equations are the mathematical expressions of conservation of mass and momentum. Continuity equation (or mass conservation equation) of a fluid flow is in the form of equation (1) (19).

$$\frac{\partial \rho}{\partial t} + \frac{\partial}{\partial x_i}(\rho u_i) = 0 \qquad (1)$$

Navier-Stokes equations are the momentum equations governing the flow of viscous Newtonian fluid, and their tensor form in Cartesian coordinates is expressed with equation (2) (20).

$$\rho\left(\frac{\partial u_i}{\partial t} + u_j\frac{\partial u_i}{\partial x_j}\right) = -\frac{\partial P}{\partial x_i} + \frac{\partial \tau_{ij}}{\partial x_j} + \rho g_i$$

(2)

In the above equation, the left side terms represent the fluid acceleration and consist of spatial and temporal changes, and the right side term represents force per unit mass.
The standard k-ε model is a quasi-experimental model based on two transport equations for the turbulent kinetic energy (k) and the turbulent dissipation (ε). The transport equation for k is obtained from the explicit equation and transport equation for ε is obtained using physical reasoning. The k-ε model assumes that flow is fully turbulent and the effect of molecular viscosity is negligible. In this model, K and ε transport equations are defined as equations (3) and (4) (21).

$$\frac{\partial(\rho K)}{\partial t}+\frac{\partial(\rho K u_i)}{\partial x_i}=\frac{\partial}{\partial x_j}\left[\left(\mu+\frac{\mu_t}{\sigma_k}\right)\frac{\partial K}{\partial x_j}\right]+G-\rho\varepsilon \quad (3)$$

$$\frac{\partial(\rho\varepsilon)}{\partial t}+\frac{\partial(\rho\varepsilon u_i)}{\partial x_i}=\frac{\partial}{\partial x_j}\left[\left(\mu+\frac{\mu_t}{\sigma_\varepsilon}\right)\frac{\partial \varepsilon}{\partial x_j}\right]+C_{1\varepsilon}\frac{\varepsilon}{K}G-C_{2\varepsilon}{}^{*}\rho\frac{\varepsilon^2}{K}G \quad (4)$$

In the above equations, $C_{2\varepsilon}{}^{*}=C_{2\varepsilon}+\frac{C_\mu\eta^3(1-\eta/\eta_0)}{1+\beta\eta^3}$, $\eta=\frac{SK}{\varepsilon}$, $S=(2S_{ij}S_{ij})^{0.5}$, and $S_{ij}=\frac{1}{2}(u_{ij}+u_{ji})$; μ_t is the turbulence viscosity, which is calculated by placing K (turbulent kinetic energy) and ε (turbulent dissipation) in equation (5):

$$\mu_t=\rho C_\mu\frac{K^2}{\varepsilon} \quad (5)$$

Using the average velocity gradient, turbulent kinetic energy generation G is defined with equation (6).

$$G=\mu_t\left(\frac{\partial u_i}{\partial x_j}+\frac{\partial u_j}{\partial x_i}\right)\frac{\partial u_i}{\partial x_j} \quad (6)$$

3. NUMERICAL MODELING

In this paper, flow pattern around the spur dike was investigated using the FLUENT. FLUENT is a powerful software application for analyzing fluid/heat flow in the presence of complex geometries and unstructured mesh. The unique feature of this software include the possession of an extensive database for a wide range of materials, the flexibility to work with user-defined functions (UDF), the ability to modify the mesh during analysis based on changes in the solution parameters, the use of different discretization techniques, the use of different turbulence models such as k-ε , k-ω, RSM, Spalart, Allmaras, DES, LES and their derivatives, and the possession of a wide range of boundary conditions. Fluent's use of unstructured mesh reduces the solution time, simplifies the geometric modeling and mesh generation process, and allows the user to model more complex objects. It should however be noted that the basic geometry and mesh are best to be developed outside Fluent using software applications such as Gambit.

4. MODEL PREPARATION

The experimental result of Hosseini (2012) was used for validity assessment. In that laboratory study, spur dike was made of Plexiglas, had a wing and web length of 9 cm, and had a semi-circular nose with a thickness of 1 cm. These experiments were conducted using attracting spur dikes placed in series at 120 degrees angle with the flow direction. The distance between the spur dikes was 31.5 cm. The flume had a length of 7 m, the width of 60 cm, and depth of 12.8 cm. The inflow had a velocity of 0.33 meters per second, which resulted in the Froude number of 0.3. In the present study, the basic geometry was created with the software Gambit, and the area around the spur dikes was given a finer mesh to accommodate for erratic changes of flow velocity in those sections. The best mesh size was determined by trial and error, and the geometry was developed with a total of 211952 elements. Different sections were modeled using the walls and inflow and outflow boundary conditions. Since the changes of water level were negligible, the water surface profile was ignored to prevent the emergence of two phases in the model. Turbulent flow was modeled using the k-ε model with constant coefficients given in Table 1.

Table 1. Constant coefficients of the k-ε turbulence model

$C_{2\varepsilon}$	$C_{1\varepsilon}$	C_μ	σ_ε	σ_k
1.92	1.44	0.09	0.76923	1

The validity of the obtained longitudinal and transverse velocity components around spur dikes in the near-bed levels was examined. Velocity distribution around the series of spur dikes in the laboratory study of Hosseini and the present study are shown in Figure 1 (a-d). As can be seen, dike structure narrows the passage, so the flow rate is higher in front of dikes that it is in other areas. The greatest longitudinal velocity component can be seen in front and

between the wing of the first dike and the wing edge of the second dike. Longitudinal velocity component is greater in front the wing of the first dike than it is in front of the second and third dikes, and it is greater in front the wing of the second dike than in front the third dike. Because of the narrowing, the edge of the upper wing of the first dike exhibits a strong positive cross-flow, which gets weaker at higher levels. The area between the spur dikes exhibits a reverse flow creating negative transverse velocity, and area of this region increases with elevation. In both flow levels, the positive cross-flow is stronger between the first and second dikes than between the second and third dikes.

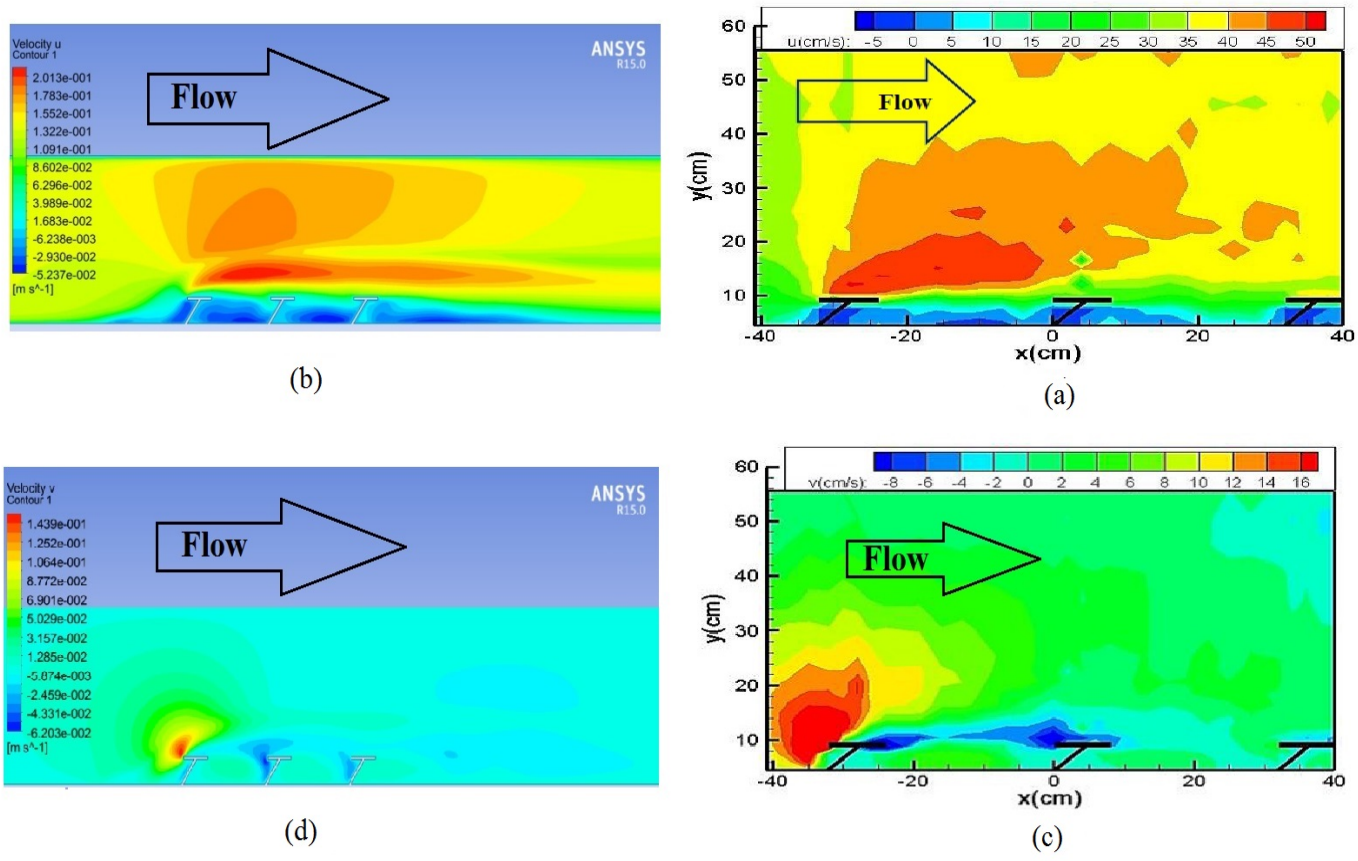

Figure 1. Velocity distribution around spur dikes placed in series at the elevation of Z = 0.5 cm from the bed a) Longitudinal velocity reported by the experimental study, b) longitudinal velocity obtained in the present study by modeling, c) transvers velocity reported by the experimental study, d) transvers velocity obtained in the present study by modeling

The numerical results obtained with the Fluent showed a good agreement with the experimental results, and this demonstrated the good ability of this software to simulate the flow pattern around T-shaped spur dikes placed in series within a straight channel. Next, the effect of geometric parameters of the spur dike on the flow pattern was evaluated by simulating the flow with different values for dike length and spacing between the consecutive dikes. The effect of dike length was simulated for two lengths of 9cm and 15cm, the latter being the maximum dike length (25% of the channel width), and the effect of distance between dikes was simulated with values of 22.5cm and 33.5cm, which are, respectively, 2.5 and 3.5 times the length of spur dike.

5. RESULTS

The effect of dike length on flow lines around three attracting spur dikes placed in series near the channel bed is shown in Figure 2. As Figure 2 (a) and Figure 2 (b) show, the increase in dike length increases the flow diversion from the wing edge of the first dike. There is a small eddy (rotating) flow in the area behind the first spur dike, but this flow disappears with the increase of dike length. There is another eddy flow in the area between the first and second spur dikes, and as the dike length increases, the core of this eddy flow moves toward the first dike and wall of the channel. There is also an elliptical eddy flow after the third dike, which grows with the increase of dike length.

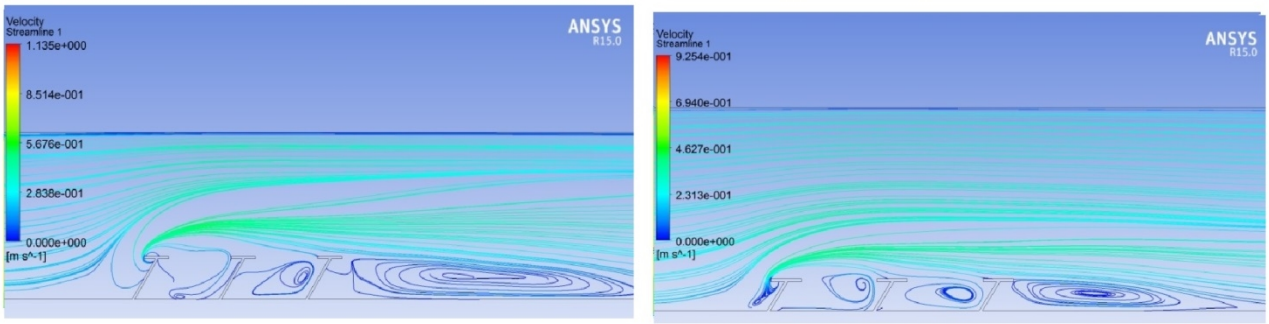

(b) (a)

Figure 2. the effect of dike length on the flow pattern for dikes placed with spacing of D = 31.5 cm, a) 9-cm dike placed at 0.5cm distance from the bed b) 15-cm dike placed at 0.5cm distance from the bed

The effect of dike length on longitudinal and transverse flow velocities around three attracting spur dikes placed in series near the channel bed is shown in Figure 3. According to this figure, the increase of dike length narrows the channel and compresses the flow lines, and this significantly increases the peak longitudinal flow velocity in the area between the first and second spur dikes. On the other hand, the increase of dike length leads to a formation of a slow reverse flow behind the first dike. As the dike length increases, positive component of transvers velocity at the wing edge of the first dike exhibits a sharp increase, which signifies a severe flow diversion. The negative components of this parameter increases between the second and third dikes.

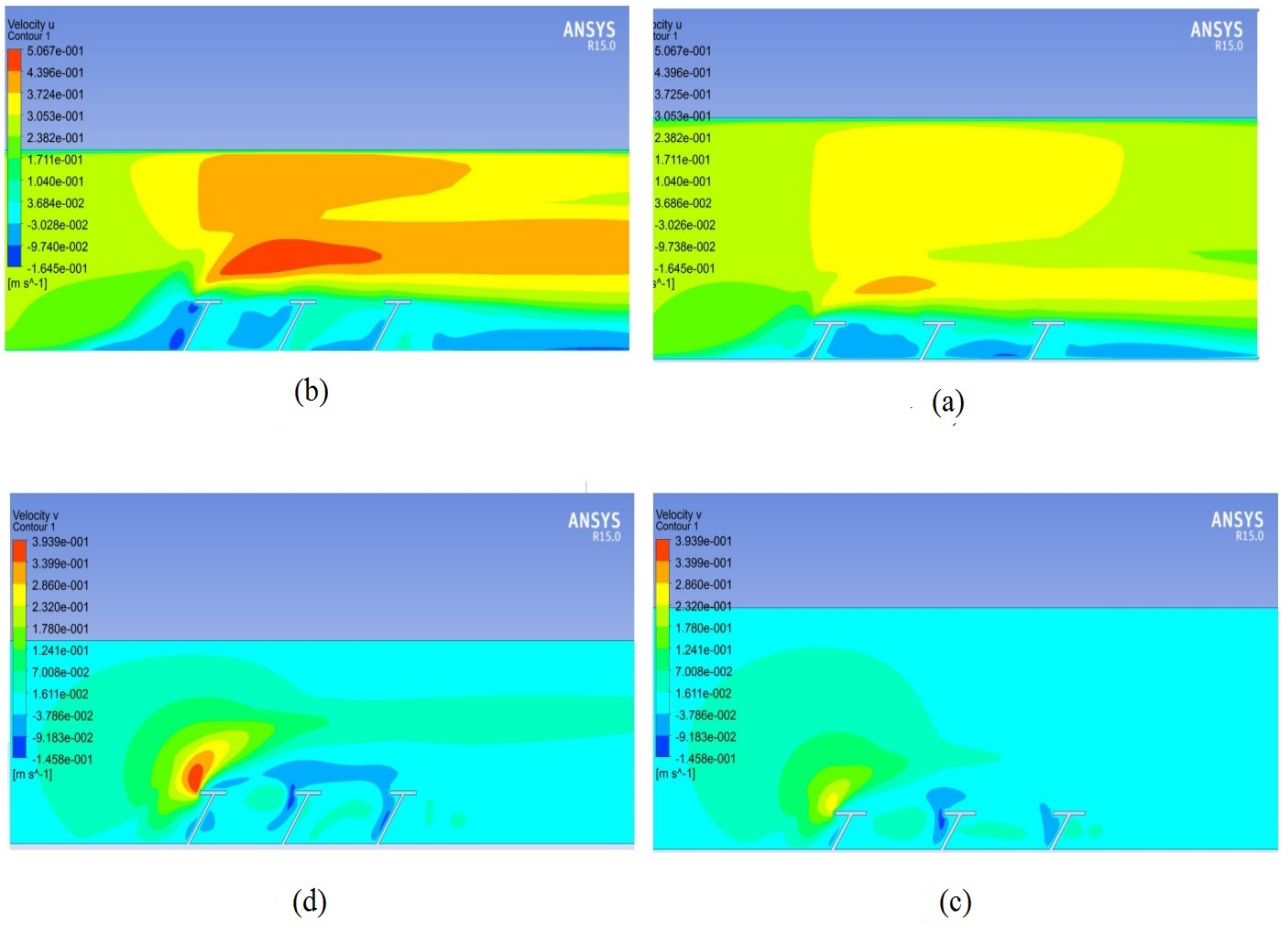

(b) (a)

(d) (c)

Figure 3. the effect of dike length on velocity distribution at the elevation of Z=0.5cm from the bed, a) longitudinal velocity resulting from 9-cm dikes placed 31.5cm apart b) longitudinal velocity resulting from 15-cm dikes placed 31.5cm apart c) transvers velocity resulting from 9-cm dikes placed 31.5cm apart d) transvers velocity resulting from 15-cm dikes placed 31.5cm apart

Figure 4 shows the effect of distance between dikes on the flow pattern around three attracting spur dikes placed in series near the channel bed. According to Figure 4 (a, b), the increase in the dike spacing has no effect on flow diversion from the wing edge of the first spur dike. The Figure 4 (a) shows the eddy flow present in the area between the first and second dikes. As the dike spacing increases, the said eddy flow turns into two eddy flows,

one between the wings and the other between the webs of the dikes.

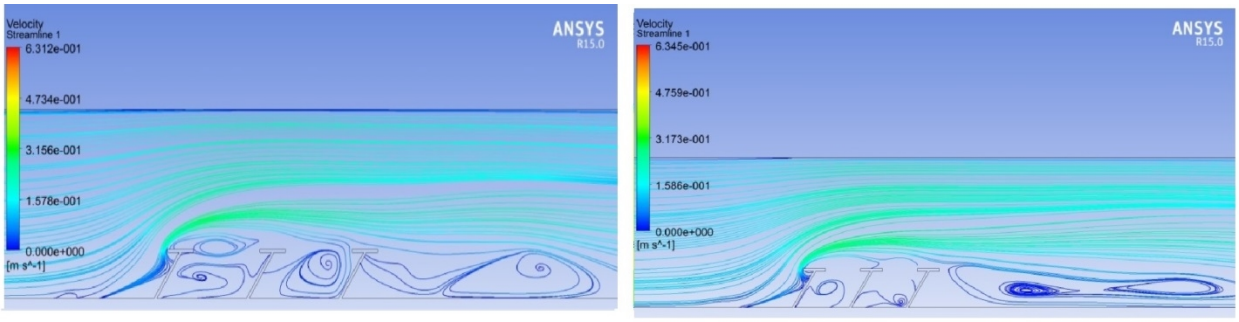

(b) (a)

Figure 4. The effect of dike spacing on the flow pattern, a) 15-cm dikes placed 22.5cm apart at 0.5cm distance from the bed b) 15-cm dikes placed 31.5cm apart at 0.5cm distance from the bed

In the area between the second and third dikes, eddy flow grows in size and moves away from the wall toward the wing of the third dike. In the downstream side of the third spur dike, as the dike spacing increases, the two elliptical eddy flows turn into a single one. The effect of dike spacing on longitudinal and transverse flow velocities around three attracting spur dikes placed in series near the channel bed is shown in Figure 5. This figure shows that the increase in dike spacing has no effect on the distribution of positive longitudinal velocity, but increases the negative longitudinal velocity between the first and second dikes and decreases the negative longitudinal velocity in the downstream side of the third dike. The increase in dike spacing also has no effect on the distribution of positive transvers velocity but increases the negative longitudinal velocity in the upstream side of the third dike.

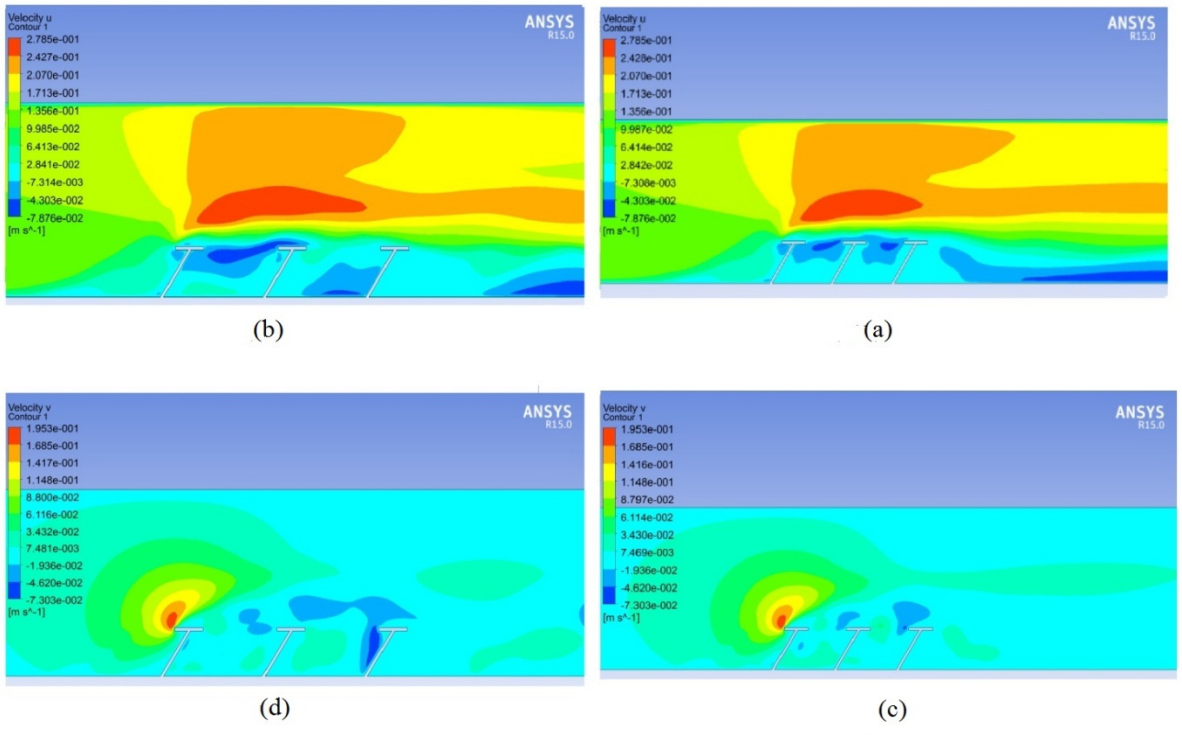

Figure 5. the effect of dike spacing on velocity distribution at the elevation of Z=0.5cm from the bed, a) longitudinal velocity resulting from 15-cm dikes placed 22.5cm apart b) longitudinal velocity resulting from 15-cm dikes placed 31.5cm apart c) transvers velocity resulting from 15-cm dikes placed 22.5cm apart d) transvers velocity resulting from 15-cm dikes placed 31.5cm apart

6. CONCLUSION

In this study, flow pattern and velocity distribution around three attracting T-shaped spur dikes placed in series were simulated with the FLUENT, to assess the effect of geometrical parameters such as dike length and spacing on the flow pattern. The results showed that the increase of dike length narrows the channel and compresses the flow lines, and thereby increases the peak longitudinal flow velocity in the area between the first and second dikes, and also enlarges the eddy flow in the downstream side of the third dike. Increasing the dike spacing triggers no change in flow diversion, so it has no significant effect on the peak longitudinal flow velocity around the dike edge. However,

increasing this spacing changes the pattern of eddy flows in the area between the dikes and in the downstream side of the last dike, and leads to the formation of larger vortices. According to the obtained results, flow pattern was affected more by the increase in dike length than by the increase in dike spacing.

FUNDING/SUPPORT

Not mentioned any Funding/Support by authors.

ACKNOWLEDGMENT

Not mentioned any acknowledgment by authors.

AUTHORS CONTRIBUTION

This work was carried out in collaboration among all authors.

CONFLICT OF INTEREST

The author (s) declared no potential conflicts of interests with respect to the authorship and/or publication of this paper.

REFERENCES

1. Fazli M, Ghodsian M, Neyshabouri SAAS. Scour and flow field around a spur dike in a 90 bend. International Journal of Sediment Research. 2008;23(1):56-68.
2. Elawady E, Michiue M, Hinokidani O. Movable bed scour around submerged spur-dikes. Proceedings of Hydraulic Engineering. 2001;45:373-8.
3. Vaghefi M, Ghodsian M, Salehi Neyshaboori S. Experimental study on the effect of a T-shaped spur dike length on scour in a 90 channel bend. Arabian Journal for Science and Engineering. 2009;34(2):337.
4. Vaghefi M, Shakerdargah M, Akbari M. Numerical investigation of the effect of Froude number on flow pattern around a submerged T-shaped spur dike in a 90 bend. Turkish Journal of Engineering and Environmental Sciences. 2015;38(2):266-77.
5. Safarzadeh A, Salehi Neyshabouri SAA, Zarrati AR. Experimental investigation on 3D turbulent Flow around straight and T-Shaped groynes in a flat bed channel. Journal of Hydraulic Engineering. 2016;142(8):04016021.
6. Mehraein M, Ghodsian M, Khosravi MM. Experimental study of submergence effect on turbulent parameter around spur dike located in a 90 bend. 2016.
7. Kuhnle R, Jia Y, Alonso C. Measured and simulated flow near spur dikes. US-China workshop on advanced computational modeling in hydroscience and engineering. Oxford, MS, USA; 2005.
8. Kuhnle RA, Jia Y, Alonso CV. Measured and simulated flow near a submerged spur dike. Journal of Hydraulic Engineering. 2008;134(7):916-24.
9. Kuhnle RA, Alonso CV, Shields Jr FD. Local scour associated with angled spur dikes. Journal of Hydraulic Engineering. 2002;128(12):1087-93.
10. Salamatian S, Forghani M, Tabarestani MK. Flow Pattern and Stress Distribution around Three Spur Dike in Ninety Degree Bend. International Journal of Engineering and Technology. 2016;8(6).
11. Kumar M, Malik A. 3D Simulation of Flow around Different Types of Groyne Using ANSYS Fluent. Imperial Journal of Interdisciplinary Research. 2016;2(10).
12. Karami H, Basser H, Ardeshir A, Hosseini SH. Verification of numerical study of scour around spur dikes using experimental data. Water and environment journal. 2014;28(1):124-34.
13. Yazdi J, Sarkardeh H, Azamathulla HM, Ghani AA. 3D simulation of flow around a single spur dike with free-surface flow. Intl J River Basin Management. 2010;8(1):55-62.
14. Duan JG, He L, Fu X, Wang Q. Mean flow and turbulence around experimental spur dike. Advances in Water Resources. 2009;32(12):1717-25.
15. Tang X, Ding X, Chen Z. Large eddy simulations of three-dimensional flows around a spur dike. Tsinghua Science & Technology. 2006;11(1):117-23.
16. Uijttewaal WS. Effects of groyne layout on the flow in groyne fields: Laboratory experiments. Journal of Hydraulic Engineering. 2005;131(9):782-91.
17. Fei-Yong C, Ikeda S. Horizontal separation flows in shallow open channels with spur dikes. Journal of Hydroscience and hydraulic Engineering. 1997;15(2):15-30.
18. Osman AM, Thorne CR. Riverbank stability analysis. I: Theory. Journal of Hydraulic Engineering. 1988;114(2):134-50.
19. Barnjani SHR, Safari A, Mofrad BM. Numerical Simulation of Turbulence and Flow Velocity Distribution Around the Spur Dike Using FLUENT. Journal of Civil Engineering and Materials Application. 2017;1(1):28-32.
20. Safari A, Mofrad BM, Barnjani SHR. Investigating LES Turbulence Model in Modeling the Velocity Distribution Around the Hydraulic Structure Using ANSYS. Journal of Civil Engineering and Materials Application. 2017;1(2):33-8.
21. Mofrad BM, Barnjani SHR, Safari A. Modeling of Turbulent Flow Due to the Dam Break Against Trapezoidal Barrier. Journal of Civil Engineering and Materials Application. 2017;1(1):22-7.